ISSN: 1687-1006 p
ISSN: 2682-3640 e

The Egyptian International Journal of Engineering Sciences and Technology

https://eijest.journals.ekb.eg/

Vol. 45 (2024) 63–90

DOI: 10.21608/EIJEST.2023.210866.1229

An Analysis of Marine Vessel Manoeuvrability Using a Modified Linear Quadratic Regulating Controller Design to Enhance Performance

Oluseye Adebayo Owolabi, Olatunbosun Ajayi, Sunday Ayoola Oke*

Department of Mechanical Engineering, University of Lagos, Lagos, 101017, Nigeria

ARTICLE INFO

Article history:

Received 14 May 2023
Received in revised form
08 July 2023
Accepted 29 July 2023
Available online 29 July
2023

Keywords:

Controller design
Stability
Measurement
ship vessel
manoeuvring

ABSTRACT

Ship stability is one of the most valuable operational situations of ships and provides essential information on the weather conditions, safety and control ability of the ship. To guarantee a ship's sustainability, there is an urgent need to analyze and apply the results of vessel manoeuvring dynamics and establish the controller's design thereby assuring the ship's performance. To address the problem, this study introduces a modified form of the linear quadratic regulator (LQR) controller design to control and influence the random fluctuations in the system state measurements stable results were obtained in the various cases that were tested. The controller was robust enough to deal with measurement noise under varying circumstances. Considering the vessel's turning radius bend of 300 millimeters and the completion of a full turn in 3.5 minutes, the performance of the controller tested in a real situation reveals that increasing the controller gains through the values of the Q and R (quadratic regulator) matrices affected different parts of the response. Furthermore, from the simulation, for every 1 second of simulation time, we have 20.85 seconds of real-time. The real-time plots provided are 0.24 seconds of simulation time. Also, the higher value of the Q matrix coefficients stimulated a faster response since the feedback gain increases commensurately. The result is significant as it enables naval architects to easily manoeuvre vessels in a predictable way which is the effect of this controller design.

1. Introduction

Ship vessels are critical elements of the maritime industry [1, 2, 3]. According to the Nigerian government, increased investments are to be made to expand to service and capacity of the major players in the marine industry [4]. Interestingly, the coastline of Nigeria runs roughly 853 km at the boarder of Atlantic Ocean, according to Ateme [5]. Furthermore, Ateme [5] declared that Nigeria is within the Gulf of Guinea area with substantial resources in the maritime area of roughly 46,000 km^3 and it is a strong base for economic prosperity. Therefore, ship vessel expansion has excellent prospects [5]. For ship

* Corresponding author. Tel.: +234-080-581-791-90
E-mail address: saoke01@gmail.com.

vessels, the control of marine vessel manoeuvrability is the most important aspect of safety sustenance [6, 7, 8]. Effective control means assuring the stability of the shipping vessel [9]. So efforts are urgently required to analyse and improve the control elements of the shipping vessel regarding manoeuvrability issues. Unfortunately, the paucity of skilled manpower in this area and less research conducted makes the concrete determination of control and manoeuvrability very challenging. In addition, the economy of the marine industry is recently affected by the global COVID-19 pandemic experience, which shut off activities across the globe for a long time [10, 11, 12]. This is also coupled with the global economic meltdown in which Nigeria has been greatly affected [13]. The so-called ship vessel manoeuvrability concerns the initial turning ability, which is maintaining a high turning speed, yaw assessment capability and a quick stoppage ability to turn motion [14].

From a practical viewpoint, ship vessel manoeuvrability has remained a substantial challenge faced by naval architects [14]. Naval architects steer a straight course of the ship by using a large rudder area [14]. The architect sets the rudder angle at zero for the vertical stabilization of the fins and also puts it at different angles, creating large swinging moments essential for good turning [14]. The complexity of ship vessel manoeuvrability makes the traditional manual or the experience of the naval architect yield low control efficiency [15]. The extremely difficult optimisation of the manoeuvrability indices seriously restricts the enhancement of the efficiency of the manoeuvrability [15, 16]. Therefore, the trend is to achieve optimal manoeuvrability of ship vessels.

Moreover, theoretically, studying the ship vessel manoeuvrability problem is exceptionally challenging [15, 16]. However, to simplify the situation, manoeuvrability could be described as a 6-degree-of-freedom multiple input, multiple output dynamic system [17, 18, 19]. Then the state space analysis is deployed for optimal control [20, 21]. Nonetheless, according to the in-depth research recently, the academic and marine fields reveal that the results on the ship vessel manoeuvrability highly concentrated on human initiatives and experience and there is no mature technical solution to analyze ship vessel manoeuvrability where the influence of random fluctuations in the system state measurements could be monitored [14].

In this article, a modified form of the linear quadratic regulator controller design is proposed to control and influence the random fluctuations in the system state measurements. The main contributions of this article are as follows:

1. A method based on a linear quadratic regulator-based control system is proposed to stabilize an unstable vessel and track the reference inputs with satisfactory performance.
2. The Q and R matrices are considered in a steady-state solution to the matrix algebraic Riccati equation.
3. The method enables naval architects to design unstable hull forms, which are generally easier to manoeuvre.

The objectives of this work are three-fold: First is to develop a linear state-space marine vessel model with manoeuvrability; second is to design a Linear Quadratic Regulator (LQR) based control system for stabilizing the model and tracking a required response; and third is to verify the performance of the controller with varying inputs. Section 2 presents a review of the literature on ship dynamics and modelling methods. This section also focuses on control system design using the Linear Quadratic Regulator approach. Section 3 presents the problem definition and the design methodology for solving the problem. In section 4, a summary of relevant results and guides to their interpretation are presented. The results are analysed and discussed. Section 5 is the conclusion, including recommendations and identifies open areas of research.

2. Literature review

In the literature concerning the present subject, some efforts have been made on manoeuvring and controlling ship vessels. These efforts are reviewed here to create a basis for the identification of gaps that strengthens the pursuit to analyse the control of ship vessels discussed in the present work. Furthermore, given the increasing pressure to be safety aware offshore and the increasingly difficult opportunities to repair and/or replace components or the whole ships, it is unsurprising that ship manoeuvring is increasingly being scritunized but the knowledge accumulation in the area is still relatively low. Ship manoeuvring is a clever idea that embraces many aspects of human endeavour: mechanical engineering, wind studies, electrical controls, water resources engineering among others. Therefore a detailed account of the literature is given in the present study and follows.

2.1 Manoeuvrability and controllability of vessels

In terms of maneuvering, Piaggio et al. [9] proposed a new model to evaluate the heel influence in maneuvering in surface vessel, using an extended twin-screw model using the heeling angle as an input that incorporates the zig-zag IMO margins and turning. Wang et al. [23] modelled the dynamics of shipping vessels with a knowledge transfer policy for the adaptation of domain knowledge to a focused ship. A data-driven function was the backbone of the model coupled with a featured vector and the whole model predicts the trajectories of maneuvering in diverse situations. To clarify Table 1 lists the previously discussed articles on manoeuvrability and controllability of vessels and some details about the work in comparison with the present study. To compare the present study with the previous ones, the current study uniquely and innovatively deploys a modified version of the linear quadratic regulating controller design to establish the manoeurability of marine vessels which provided a rough controller capable to tackle the measurement noise subjected to diverse situations.

Table 1. A summary of some studies representing manoeurability of ship vessels

Reference	Method	Essential factors
Piaggio et al. [9]	Modified twin-screw model	Kijima's single-screw container vessel model, heeling angle, transverse stability, loading conditions
Wang et al. [23]	Ship maneuvering model	knowledge transfer strategy model, data-driven transfer function, feature vector, reflective ship state, transfer ship predictions
Wang et al. [15]	Deep neural networks oriented maneuvering model	Data driven method, voyage data recorder, duration of ship voyage
Liu et al. [22]	Network control system	Positioning, velocity, altitude, time
Wei et al. [24]	Recognition algorithm	Automatic identification system, joint probability density function, ship traffic rules
Lu et al. [25]	Computational fluid dynamics and empirical models	Advanced coefficients, rudder angles, polynomial regression method
The present paper	Modified linear quadratic regulating controller	Yaw response, matrix weights, controller performance indicator

Moreover, many motions characterize a vessel's overall motion. There are motions induced by environmental factors such as wind and waves, motions due to the propulsive devices, motions due to the cargo if, for example, the vessel is carrying a large amount of liquid with a free surface, and there are motions due to control elements such as rudders and fins. Manoeuvring involves the motions of a ship as a result of action taken by some control mechanism e.g. the autopilot or the helmsman [26]. It can be defined as a controlled change of course and its characteristic time length spans over a few minutes [26]. This time length also serves to distinguish manoeuvring problems from seakeeping ones which have characteristic time lengths of a few seconds. Seakeeping problems involve the motion of the vessel in waves [26]. Traditionally, manoeuvring problems have been studied on the assumption that the vessel is operating in calm water conditions though for modern applications seakeeping characteristics have been incorporated in the vessel models to give more realistic results [27].

In considering the manoeuvrability of vessels there are certain important considerations as presented in Papoulias [26]. These are course stability, turning, slow speed operation and stopping. Course stability refers to the ability of a vessel to maintain a straight course without any control input while turning involves a change of course due to control inputs. Slow speed operation was earlier discussed, where it was mentioned that the rudder loses its effectiveness as a primary control device at low speeds and stopping generally involves bringing the vessel to a halt by a combination of methods which could involve the propeller reversal. Of the considerations mentioned above, turning and course stability have very differing requirements. A very stable vessel will be hard to turn. However, an unstable vessel gets turned easily. Coupled with this, it may turn itself as a result of external disturbance. Generally it is desirable for a vessel to be able to keep a straight course without control inputs (fixed course stability) moreover, by developing fuller vessels as well as open sterns, which enhances propeller-generated vibration, course unstable vessels have subsequently been developed and operated with success for a while now [26].

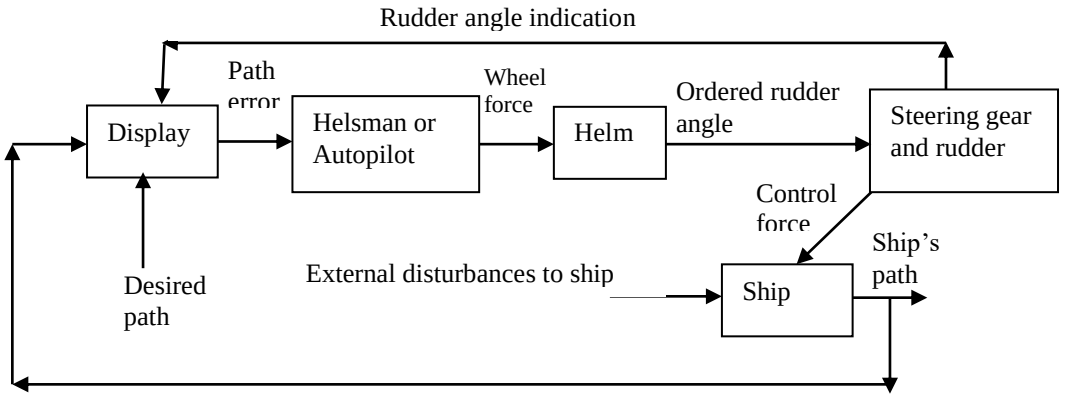

Figure 1: Ship controllability and manoeuvrability loop [26]

For this work the focus will be on the ship block (Figure 1) and its response to signals which may be control inputs or external disturbances. The autopilot block is also considered from a control systems perspective to improve the response of the vessel to inputs and for stabilization. The modern approach to manoeuvring involves a combination of classical manoeuvring and seakeeping. To achieve this, the models for ship motion control system design generally use superposition of motion or forces [27]. The most popular is the motion superposition method (Figure 2) which has an easier implementation but has the drawback that it cannot be used for cases where there are parameters in the study that involve the effect of one vessel on the other i.e. multibody system interactions and the manoeuvring part does not incorporate fluid memory (viscous) effects that are included in every real fluid. Indeed, the radiation forces due to the frequency-dependent mass and damping of the ship are only considered in the seakeeping model. This results in miss-modelled dynamics, which are of interest for ship motion control in a seaway [27].

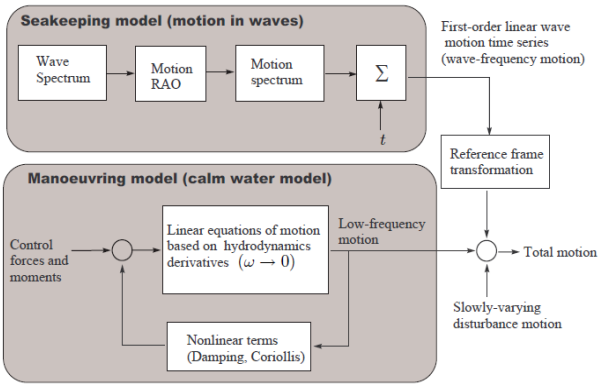

Figure 2. Motion superposition model of a marine vessel [27].

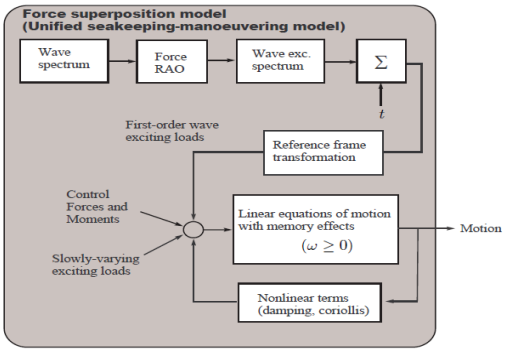

Figure 3. Force superposition model of a marine vessel [27]

The force superposition model (Figure 3) is generally more accurate in simulating ship motion in a variety of environments but is not as easily adaptable to control system design.

2.2 Modelling ship dynamics

In Figure 4, two major reference frames are introduced for the description of vessel motions. A vector in the inertial frame is denoted $\overline{\mathrm{X}}$, while that in a body reference frame is denoted by $\overline{\mathrm{X}}_0$. The body-referenced frame moves along with the vessel and is more convenient for representing the vessel's motions thus motions are usually referred to it. The two frames in the general case have entirely different origins and could also have different orientations. It is necessary to have a means of transforming motions from one frame to the other. To achieve this, the Quaternions and Euler angles methods could be used [27].

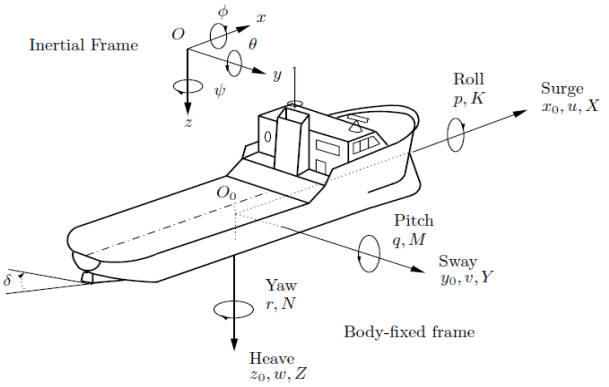

Figure 4: Standard notation and sign conventions for ship motion description (SNAME, 1950 [28])

In Figure 4, the symbols P, k, q, H, r and N are the ship's motion variables. Moreover, quaternions are numbers with special properties that make them very elegant for dealing with spatial rotations [29]. Quaternions are used as mathematical notations to denote orientations and rotations of objects. Users in robotics, orbital mechanics of satellite, computer graphics and global navigation have widely used quaternions because of their efficiency, compactness and stability benefits compared with matrices [30]. They however require a very high level of mathematical abstraction to deal with. Euler angles are preferred in this context because of their relative ease of application and intuitiveness; successive rotations correspond to the traditional notions of roll, pitch and yaw. The main shortfall of the method is that there are specific values for which the transformation exhibits discontinuities.

The Euler angle approach involves applying a series of successive rotations to the axes of a reference frame and concatenating the rotation matrices [31]. To find the coordinate of a point fixed

in inertial space referenced to a rotated body frame we require a transformation in the form of a 3 x 3 matrix derived through successive rotations of the three Euler angles. At the initial point, the coordinates are assumed coincident and identical i.e. $\vec{x}_0^0 = \vec{x}$. After the sequence of rotations, the transformation matrix is found as,

$$\vec{x}_0 = \begin{bmatrix} \cos\theta\cos\phi & \cos\theta\sin\phi & \sin\theta \\ -\cos\psi\sin\phi + \sin\psi\sin\theta\cos\phi & \cos\psi\cos\phi + \sin\psi\sin\theta\sin\phi & -\sin\psi\cos\theta \\ \sin\psi\sin\phi + \cos\psi s\theta\cos\phi & -\sin\psi\cos\phi + \cos\psi\sin\theta\sin\phi & \cos\psi\cos\theta \end{bmatrix} \vec{x},$$

or $$\vec{x}_0 = R(\phi, \theta, \psi)\vec{x} \quad (1)$$

The transformation matrix $R(\phi, \theta, \psi)$ is orthonormal i.e. its transpose is equal to its inverse and this representation of R is universal to all representations of orientation. In the general case of non-coincident origins, we can write first:

$$\vec{x} = R^T \vec{x}_0 \quad (2)$$

and then

$$\vec{x} = \vec{x}_{0,0} + R^T \vec{x}_0 \quad (3)$$

where $\vec{x}_{0,0}$ is the coordinate of the body referenced frame expressed in inertial coordinates. It is also desired to have a mapping for transforming the rate of change of the Euler angles into the angular velocity of the body. This is obtained as,

$$\frac{d\vec{E}}{dt} = \begin{bmatrix} 1 & \sin\psi\tan\theta & \cos\psi\tan\theta \\ 0 & \cos\psi & -\sin\psi \\ 0 & \sin\psi/\cos\theta & \cos\psi/\cos\theta \end{bmatrix} \vec{\omega} \quad (4)$$

$$= \Gamma(\psi, \theta, \phi)\vec{\omega}$$

The matrix $\Gamma(\psi, \theta, \phi)$ is the required mapping that maps $\vec{\omega}$ to the rate of change of Euler angles $\frac{d\vec{E}}{dt}$.

Because of division by cosθ, there are singularities at $\theta = \frac{\pi}{2}, \frac{3\pi}{2}$ and these should be avoided, usually by choosing the orientation such that the angles are not on the yaw axis (see Appendix for the derivation of results).

Vessel Motions

In general, a ship is described as a rigid body with motions in six (6) degrees of freedom (6DOF). These involve three translations: surge, sway and heave corresponding to the x_0, y_0 and z_0 axis and three rotations: roll, pitch and yaw about these same axes respectively (see Figure 4). From calm water manoeuvring assumptions, the motions are assumed to be predominant in surge, sway and yaw. The descriptions of the body's motion can be done by Newton's second law. We define the inertial frame as (x_0, y_0, z_0) for convenience and the vessel-referenced frame as (x, y, z). From Newton's second law in the inertial frame:

$$\left.\begin{aligned} m\ddot{x}_0 &= X_0 \\ m\ddot{y}_0 &= Y_0 \\ I_z\ddot{\psi} &= N \end{aligned}\right\} \quad (5)$$

where X_0 – total force x_0 direction
Y_0 – total force in y_0 direction
N – turning moment around z_0 axis
m – m_{6x6} ship/vessel mass
I_z – the mass moment of inertia about z_0
ψ - yaw angle wrt x_0 axis

Using the body-referenced coordinate system; we can carry out the following transformations.

$$\left.\begin{aligned} X &= X_0\cos\psi + Y_0\sin\psi \\ Y &= -X_0\sin\psi + Y_0\cos\psi \end{aligned}\right\} \quad (6)$$

$$\left.\begin{aligned} \dot{x}_0 &= u\cos\psi - v\sin\psi \\ \dot{y}_0 &= u\sin\psi + v\cos\psi \end{aligned}\right\} \quad (7)$$

Differentiating Equation (7) and noting that $\dot{\psi} = r$ gives upon making the necessary substitutions,

$$\left.\begin{aligned} m(\dot{u} - vr) &= X \\ m(\dot{v} + ur) &= Y \\ I_z\dot{r} &= N \end{aligned}\right\} \quad (8)$$

If the axis (x, y, z) is located at some other point different from the centre of gravity, e.g. amid ships due to geometric considerations, then,

$$\left.\begin{aligned} m\left(\dot{u} - vr - x_G r^2\right) &= X \\ m\left(\dot{v} + ur + x_G r^2\right) &= Y \\ I_z\dot{r} + mx_G\left(\dot{v} + ur\right) &= N \end{aligned}\right\} \qquad (9)$$

Equation (9) can also be derived using our previous developments with rigid body dynamics. (See [26]) for details of the derivations). Centrifugal forces show up when the motions of the body are referenced to the moving axis. They do not exist for inertial coordinate frames.

The total forces X, Y and N are built up of different types of forces that act on a ship during a manoeuvre. These can be decomposed as

- Fluid forces acting on the hull due to surrounding water, subscript F.
- Control forces due to rudders, diver planes, thrusters, subscript R
- Environmental forces due to wind, current, or waves, subscript E
- Propulsive forces, T

We can then write,

$$X = X_F + X_R + X_E + T \qquad (10)$$
$$Y = Y_F + Y_R + Y_E \qquad (11)$$
$$N = N_F + N_R + N_E \qquad (12)$$

The forces represented by Equations (10), (11), and (12) can be estimated by some methods. Prominent among these are [32]:

- Module square expansion
- Taylor series expansion (linear and non-linear)

Taylor series methods involve the expansion of each of the forces as a Taylor series. Depending on the degree of accuracy required, higher-order expansion terms are either retained or dropped. Reviews of the linear and non-linear Taylor series expansions for the force estimation are provided next.

2.2.1 Linear models

For the expansion, only linear terms or first-order derivatives are considered under the linear vessel dynamics approximation. This is suitable for calm water, low wave frequency manoeuvres and moderate speeds. The fluid or hydrodynamic forces, X_F, Y_F and N_F are dependent on the vessels motion and are functions of the ships velocities and accelerations relative to the water i.e.

$$X_F = X_F\left(u, v, r, \dot{u}, \dot{v}, \dot{r}\right) \qquad (13)$$
$$Y_F = Y_F\left(u, v, r, \dot{u}, \dot{v}, \dot{r}\right) \qquad (14)$$
$$N_F = N_F\left(u, v, r, \dot{u}, \dot{v}, \dot{r}\right) \qquad (15)$$

The actual functions represented by Equations (13), (14), and (15) are quite complex but the scope of the work can be derived by considering a linear Taylor's series expansion about some nominal point (U, 0, 0) where U is the vessels forward velocity along the x-axis. We can write:

$$X_F = \frac{\partial X_F}{\partial u}(u - U) + \frac{\partial X_F}{\partial v}v + \frac{\partial X_F}{\partial r}r + \frac{\partial X_F}{\partial \dot{u}}\dot{u} + \frac{\partial X_F}{\partial \dot{v}}\dot{v} + \frac{\partial X_F}{\partial \dot{r}}\dot{r} \qquad (16)$$

$$v, r, \dot{v}, \dot{r} = 0$$

$$\therefore X_F = \frac{\partial X_F}{\partial u}(u - U) + \frac{\partial X_F}{\partial \dot{u}}\dot{u} \qquad (17)$$

Even for non-zero values of v and r, due to the usual symmetry about the midplane of a vessel, the derivatives $\frac{\partial X_F}{\partial v}, \frac{\partial X_F}{\partial \dot{v}}, \frac{\partial X_F}{\partial r}$ and $\frac{\partial X_F}{\partial \dot{r}}$ are identically zero.

$$Y_F = \frac{\partial Y_F}{\partial u}(u - U) + \frac{\partial Y_F}{\partial v}v + \frac{\partial Y_F}{\partial r}r + \frac{\partial Y_F}{\partial \dot{u}}\dot{u} + \frac{\partial Y_F}{\partial \dot{v}}\dot{v} + \frac{\partial Y_F}{\partial \dot{r}}\dot{r} \qquad (18)$$

and

$$N_F = \frac{\partial N_F}{\partial u}(u - U) + \frac{\partial N_F}{\partial v}v + \frac{\partial N_F}{\partial r}r + \frac{\partial N_F}{\partial \dot{u}}\dot{u} + \frac{\partial N_F}{\partial \dot{v}}\dot{v} + \frac{\partial N_F}{\partial \dot{r}}\dot{r} \qquad (19)$$

From symmetry about the x-z plane or port/starboard symmetry, the derivatives with respect to u, $\dot{u}$ are zero. Hence we can write:

$$Y_F = \frac{\partial Y_F}{\partial v}v + \frac{\partial Y_F}{\partial r}r + \frac{\partial Y_F}{\partial \dot{v}}\dot{v} + \frac{\partial Y_F}{\partial \dot{r}}\dot{r} \qquad (20)$$

and

$$N_F = \frac{\partial N_F}{\partial v}v + \frac{\partial N_F}{\partial r}r + \frac{\partial N_F}{\partial \dot{v}}\dot{v} + \frac{\partial N_F}{\partial \dot{r}}\dot{r} \qquad (21)$$

We can make the equations less cumbersome by denoting derivatives by subscripts indicating the variable with respect to which the operation is carried out e.g. $\frac{\partial N_F}{\partial v} = Nv$

Considering the forces due to controls working, in this case, the rudder, and assuming that the rudder force is a function of the rudder angle δ and neglecting any forces due to the rate of change of the rudder angle δ i.e. steady states, we can write:

$$X_R(\delta) = X_R(0) + \frac{\partial X_R}{\partial \delta}\delta = 0 \qquad (22)$$

$$Y_R(\delta) = Y_R(0) + \frac{\partial Y_R}{\partial \delta}\delta = Y_\delta\ \delta \qquad (23)$$

And

$$N_R(\delta) = N_R(0) + \frac{\partial N_R}{\partial \delta}\delta = N_\delta\ \delta \qquad (24)$$

Neglecting environmental disturbances and propulsive forces the linearized surge, sway and yaw equations of motion are:

$$(m - X_{\dot u})\dot u = X_u(u - U) \qquad (25)$$

$$(m - Y_{\dot v})\dot v - (Y_{\dot r} - mX_G)\dot r = Y_v v + Y_\delta \delta + (Y_r - mU)r \qquad (26)$$

$$(I_z - N_{\dot r})\dot r - (N_{\dot v} - mX_G)\dot v = N_v v + N_\delta \delta + (N_r - mX_G U)r \qquad (27)$$

It can be seen that the surge Equation (25) is decoupled from the sway and yaw Equations (26) and (27). This implies that the longitudinal dynamics do not affect the turning characteristics as such. These equations represent the linearized system dynamics of a vessel and can be converted for control system design. An important feature of this linear model is the stability of the vessel which is considered next.

Stability of the Sway/Yaw System: Straight-Line Motion

Stable straight-line motion is very important in consideration of course stability or path-keeping. There are different types of stability possible and associated with marine vessels

1. Dynamic stability/straight-line stability
2. Directional stability
3. Positional stability

For a self-propelled vessel, the only kind of motion stability possible is dynamic stability. However, in the vertical plane, surface vessels also possess positional stability. It can be shown that, for stability, given a stability coefficient C,

$C = Y_v N_r + N_v (mU - Y_r) > 0$ (28)

For non-zero x_G,

$C = (N_r - mx_G U)\ Y_v - (Y_r - mU)\ N_v > 0$ (29)

This is the stability criterion. The more positive C is, the more dynamically stable the vessel is and the harder it is to turn. This is the conflicting requirement stated in Section 2.1.

2.2.2 Non-linear models

The linear analysis is valid only for small angles of attack of the rudder δ and turning rates [26]. It fails however to predict accurately the manoeuvres of directionally unstable ships (C < 0) which are in existence (usually controlled using active feedback systems) [26]. It also fails to predict the characteristics of the tight manoeuvres that most vessels are capable of performing as this requires non-linear inertial components and hydrodynamic terms. Also, under the linear assumption, the surge equation is decoupled from the sway and yaw equation. The assertion that horizontal plane motions do not affect a vessel's forward speed is not necessarily true as high-speed military vessels have a substantial speed reduction in their turning manoeuvres. The non-linear equations coupled surge to the other motions are hence predicted the speed reduction in turning [26].

Using our previous method of Taylor's series expansion, non-linear terms can be included in the equations by keeping second and third-order velocity-dependent terms in Taylor's expansion. Higher-order terms (i.e. of the order of four) are not usually included as they have insignificant effects in practice [26]. The non-linear equations of motion are presented here for completion;

$$\left.\begin{aligned}(m - X\dot u)\dot u &= f_1(u, v, r, \delta)\\ (m - Y\dot v)\dot v - (Y\dot r - mx_G)\dot r &= f_2(u, v, r, \delta)\\ (Iz - N\dot r)\dot r - (N\dot v - mx_G)\dot v &= f_3(u, v, r, \delta)\end{aligned}\right\} \qquad (30)$$

$$f_1(u, v, r, \delta) = T - R$$

$$f_1(u, v, r, \delta) = T - + \frac{1}{2}X_{vv}v^2 + \left(\frac{1}{2}X_{rr}r^2 + mX_G\right)r^2$$

$$+\frac{1}{2}X_{\delta\delta}\delta^2+\frac{1}{2}X_{vuu}(u-U)v^2+\frac{1}{2}X_{rru}(u-U)r^2$$
$$+\frac{1}{2}X_{\delta\delta u}(u-U)\delta^2+(X_{vr}+m)vr+X_{v\delta}v\delta$$
$$+X_{r\delta}r\delta+X_{vru}(u-U)vr+X_{vdu}(u-U)v\delta$$
$$+X_{r\delta u}(u-U)r\delta \quad (31)$$

$$f_2(u,v,r,\delta)$$
$$=Y_o+Y_{ou}(u-U)+Y_{ouu}(u-U)^2+Y_v v$$
$$+\frac{1}{6}Y_{vvv}v^3+\frac{1}{2}Y_{vrr}vr^2+\frac{1}{2}Y_{r\delta\delta}v\delta^2$$
$$+Y_{vu}(u-U)v+\frac{1}{2}Y_{vuu}(u-U)^2v(Yr-mU)r$$
$$+\frac{1}{6}Y_{rrr}r^3+\frac{1}{2}Y_{rvv}rv^2+\frac{1}{2}Y_{r\delta\delta}r\delta^2+Y_{ru}(u-U)r$$
$$+\frac{1}{2}Y_{ruu}(u-U)^2r+Y_{\delta}\delta+\frac{1}{6}Y_{\delta\delta\delta}\delta^3+\frac{1}{2}Y_{\delta vv}\delta v^2$$
$$+\frac{1}{2}Y_{\delta rr}\delta r^2+Y_{\delta u}(u-U)\delta+\frac{1}{2}Y_{\delta uu}(u-U)^2\delta$$
$$+Y_{vr\delta}vr\delta \quad (32)$$

$$f_3(u,v,r,\delta)$$
$$=N_o+N_{ou}(u-U)+N_{ouu}(u-U)^2+N_v v$$
$$+\frac{1}{6}N_{vvv}v^3+\frac{1}{2}N_{vrr}vr^2+\frac{1}{2}N_{r\delta\delta}v\delta^2$$
$$+N_{vu}(u-U)v+\frac{1}{2}N_{vuu}(u-U)^2v(Nr-mx_G U)r$$
$$+\frac{1}{6}N_{rrr}r^3+\frac{1}{2}N_{rvv}rv^2+\frac{1}{2}N_{r\delta\delta}r\delta^2+N_{ru}(u-U)r$$
$$+\frac{1}{2}N_{\delta rr}\delta r^2+N_{\delta u}(u-U)\delta+\frac{1}{2}Y_{\delta uu}(u-U)^2\delta$$
$$+N_{rr\delta}vr\delta \quad (33)$$

T and R represent the propulsive thrust and added resistance respectively and the terms with subscript 0 represent the effects of the propellers on the turning moment and lateral forces. The Equations (31), (32) and (33) are often referred to as the 'coefficients of the equations of motion' and are usually obtained by curve-fitting actual data. In Equation (31), the extra terms model added resistance due to the ship's turning motion and rudder action. Unless balanced by an increase in propulsive thrust, these terms will cause speed loss during turning. This model gives good correlations with experimental measurements. It is however not as easily amenable to control system design as the linear model.

2.3 Linear optimal regulator design for control system applications

In general, a vessel can be represented as a 6DOF multiple input, multiple output (MIMO) dynamical systems. Classical control system analysis has generally been focused on single input, single output (SISO) systems. For this reason, in modern control theory, state space models of systems and controller synthesis methods based on state space models have wide applications. A dynamic system containing a finite number of masses or lumped parameter equivalents may be described by ordinary differential equations in the time domain [33]. Using vector-matrix notation, an nth-order differential equation may be represented by a first-order vector-matrix differential equation reducing the complexities associated with analytical treatments of higher-order differential equations.

One particular class of control system design based on state space analysis is optimal control. In optimal control, the search for a control law for a system is achieved in a way that a particular optimality condition is attained. A function of state as well as control variables is the components of the cost functional, which is a control problem. To define an optimal control, we mean a set of differential equations explaining the paths of the control variables, which minimizes the cost functional. By using the Pontryagin's maximum principle (which is a necessary condition), or proceeding on solving the Hamilton-Jacobi-Bellman equation (which, is a sufficient condition), the optimal control can be safely derived [30] and these all belong to a class of analytic methods known as variational calculus. There are various forms of optimal control depending on the aim of the designer. Five different types have been identified in Burns [34].

1. Terminal control problem: this is to bring the system as close to the terminal point as possible within a given period.
2. Minimum-time control problem: this is to bring the system to the terminal state in the shortest time possible.
3. Minimum – energy control problem: this is to bring the system to the terminal state with the least expenditure of control energy.
4. Regulator control problem: this is to restore the system to an equilibrium state after an initial

displacement while minimizing a particular performance index.

5. Tracking control problem: this is used to cause the system to track a desired trajectory while minimizing a given performance index. It is a generalization of the regulator control problem with a constantly changing reference.

The decision on which performance index to use will depend on the type of control problem at hand and the objectives of the designer. In many cases, it is conceivable that a combination of the problems listed above may be necessary and tradeoffs might be required if there are conflicting requirements e.g. minimum - time and minimum – energy requirements might be difficult to meet simultaneously.

In general, state and control variables are usually expressed as vectors and matrices using state space formulations. The control and state matrices can then be squared and combined with weighing matrices indicating the relative importance of the state output and the control effort in what is known as a *quadratic performance index* [34].

$$J = \int_0^t (\mathbf{x}^T \mathbf{Q}\mathbf{x} + \mathbf{u}^T \mathbf{R}\mathbf{u}) dt \qquad (34)$$

J is the performance index and is always a scalar
x is the state vector
u is the control vector
Q and **R** are the state and control weighing matrices respectively and are always square and symmetric.

Quadratic performance indices are commonly used because they have the advantage of giving a linear control law of the form

$$\mathbf{u}(t) = -\mathbf{K}\mathbf{x}(t) \qquad (35)$$

K is the error gain matrix.

The linear quadratic regulator (LQR) design approach gives such an optimal control law for a linear system with a quadratic performance index (see Figure 5). Its cost functional is thought in terms of penalizing the control energy measured as a quadratic form and the time it takes the system to reach zero-state [35]. The system works by driving the output of the system to a zero state from a response to a disturbance. Once the system can function to drive the output to zero, then it can be made to achieve any other desired output [35].

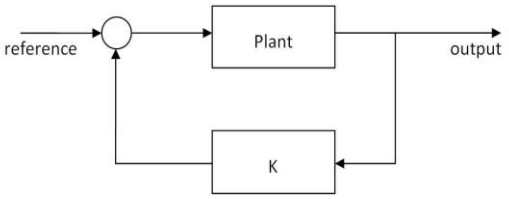

Figure 5: Linear Quadratic Regulator Design with Static Feedback Gain Matrix K

The term state regulatory problem is often used for optimal control problem established by the previous functional J(34). The corresponding solution is the Linear Quadratic Regulator (LQR) with no more than a feedback matrix gain, expressed as

$$\mathbf{u}(t) = -\mathbf{K}\mathbf{x}(t) \qquad (36)$$

K is a properly dimensioned matrix and solution of the continuous time dynamic Riccati equation (see [34] for derivations of the LQR solution).

3. Methodology

3.1 Problem definition

State space representation of the vessel

Earlier, the manoeuvring dynamics were presented as Equations (25), (26) and (27). If we write the sum of all the control forces in the X, Y and N equations as X', Y' and N', then we can remove the rudder force $Y_\delta\delta$ and moment $N_\delta\delta$ as they are already included in Y' and N'. This allows us to include effects such as those that might be due to the modern control elements. The system dynamics then become,

$$(m - X_{\dot{u}})\dot{u} = X_u u + X' \qquad (37)$$

$$(m - Y_{\dot{v}})\dot{v} + (mX_G - Y_{\dot{r}})\dot{r} = Y_v v + (Y_r - mU)r + Y' \qquad (38)$$

$$(mX_G - N_{\dot{v}})\dot{v} + (I_z - N_{\dot{r}})\dot{r} - = N_v v + (N_r - mX_G U)r + N' \qquad (39)$$

Let $\mathbf{x} = [u\ v\ r]^T$,

$\dot{\mathbf{x}} = [\dot{u}\ \dot{v}\ \dot{r}]^T$,

$\mathbf{u} = [X'\ Y'\ N']^T$,

$$\mathbf{M} = \begin{bmatrix} m - X_{\dot{u}} & 0 & 0 \\ 0 & m - Y_{\dot{v}} & mX_G - Y_{\dot{r}} \\ 0 & mX_G - N_{\dot{v}} & I_z - N_{\dot{r}} \end{bmatrix},$$

and $P = \begin{bmatrix} X_u & 0 & 0 \\ 0 & Y_v & Y_r - mU \\ 0 & N_v & N_r - mX_G U \end{bmatrix}$.

Then Equation (36), (37), and (38) can be written as,

$$\dot{x} = M^{-1}Px + M^{-1}u \quad (40)$$

Or if $A = M^{-1}P$ and $B = M^{-1}$, then

$$\dot{x} = Ax + Bu \quad (41)$$

$$y = Cx \quad (42)$$

Equation (40) is the state–space representation of the vessel and Equation (41) is the observation model. A MATLAB script is used to convert the hydrodynamic parameters into a state space model as described in the mathematical formulation. Table 2 shows the values of the hydrodynamic derivatives used in the calculations as obtained from Tristan et al. [36]. The values of the hydrodynamic parameters are usually normalized to make them amenable for use in different-sized ships with similar hull configurations.

Table 2. Values of hydrodynamic coefficients for a mariner vessel used in the calculation of the state space matrices.

Hydrodynamic coefficient	Normalised value (x 10^{-5})	Hydrodynamic coefficient	Normalised value (x 10^{-5})
X_v	184	N_r	166
X_v	-42	Y_v	748
Y_v	-1160	Y_r	9.354
Y_γ	499	N_v	4.646
N_v	264	N_r	-43.8

The values of the matrices A and B and C are

$$A = \begin{bmatrix} -0.219 & 0 & 0 \\ 0 & 1.903 & 1.025 \\ 0 & -2.653 & -1.605 \end{bmatrix}, \quad B = \begin{bmatrix} 119 & 0 & 0 \\ 0 & 50.65 & -943.4 \\ 0 & 14.04 & -943.4 \end{bmatrix}, \text{ and } \quad C = \begin{bmatrix} 1 & 0 & 0 \\ 0 & 1 & 0 \\ 0 & 0 & 1 \end{bmatrix}$$

A SIMULINK model of the system of the vessel was then developed and its response to a step input was analyzed. The responses are presented in Figure 6.

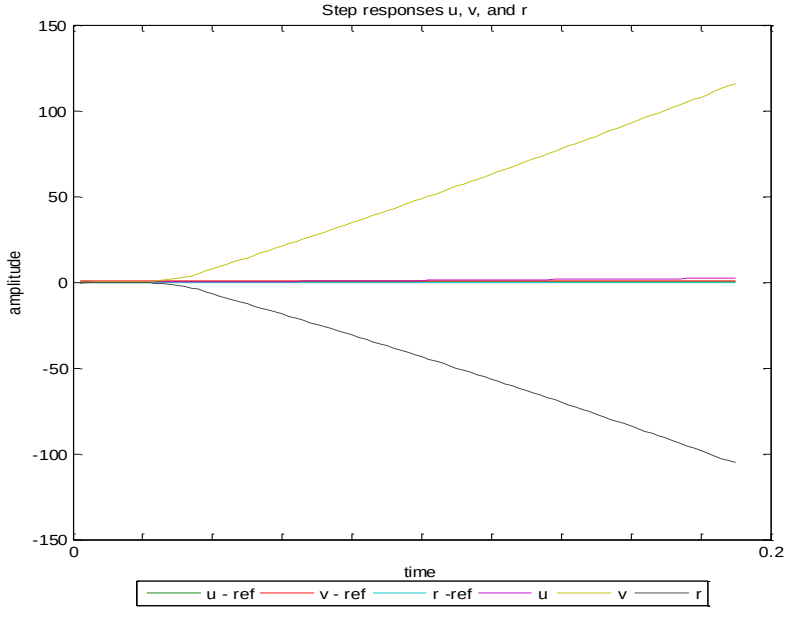

Figure 6: Step responses of mariner's vessel over 0.2 seconds showing a rapid divergence from reference values for v and r.

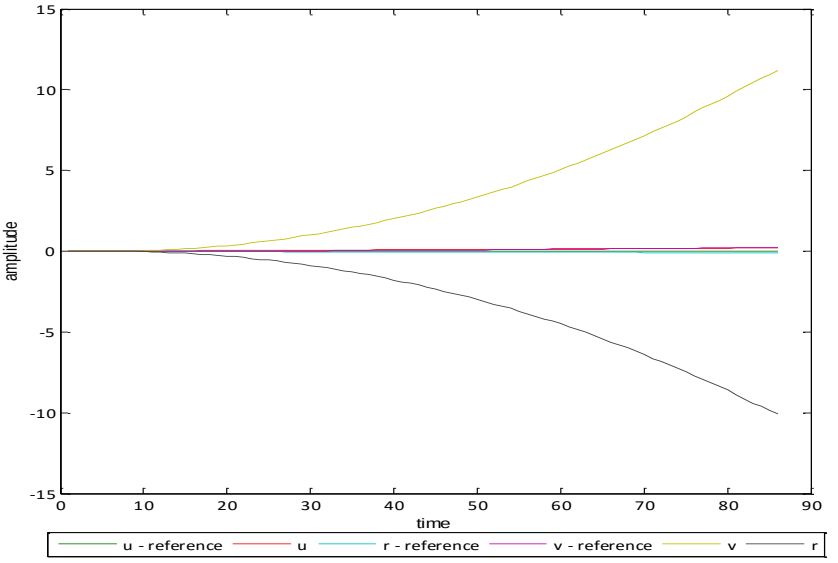

Figure 7: Ramp response of mariner's vessel for 0.2 seconds showing a divergence from reference values for v and r

Figure 6 represents the response for step inputs of 0.1, 1 and -0.5 to the three inputs u, v and r for 0.2 second. The rapid divergence of the Y and N plots indicates an unstable system. Though the mariner hull form presented in Tristan et al. [36] is generally stable, using a linear approximation yields the unstable response presented in Figure 6. Figure 7 is the ramp response of the vessel. The response is unstable for both the Y and N plots. The X plot does not show remarkable deviations because its weighing is much less than those of the other directions and control forces are generally not very large in the x – direction during manoeuvring motions. The forces are sometimes taken as zero when it is assumed that only rudder forces are in action. Also, the x – direction is uncoupled from the other two directions so the X response is independent of the Y and N responses.

As discussed earlier, though course stability is desirable, it is possible to operate an unstable vessel as long as active feedback is employed [26]. A design for an optimal controller is presented next in Section 3.2.

3.2 Control system design and Application

For a multiple input, multiple outputs (MIMO) system such as this, there are many types of multivariable controllers available for stabilizing the output [34]. Some of them are

- State Feedback Control (SFC)
  - Robust Eigenstructure Assignment (Direct Pole Placement)
  - Linear Model Reference Control
  - Optimal Control (Linear Quadratic Regulator)
  - Adaptive Control (Minimal Control Synthesis)
- State Feedback Control with Integral Action (SFCIA)
- Luenberger Observer
- Output Feedback Control (OFC)
- Output Feedback Control with Integral Action (OFCIA)

For this work, the optimal control approach is used. A review of the Linear Quadratic Regulator (LQR) was already provided in Section 2.2, but for tracking performance as opposed to regulator performance, a modification is made to the block diagram of Figure 2.5. Such an arrangement is shown in Figure 8 and is known as a Linear Quadratic Tracker [34].

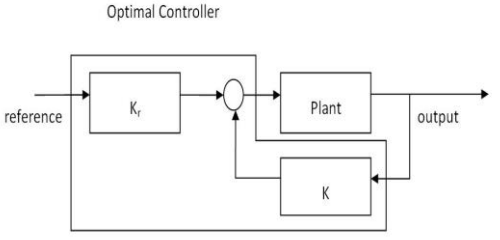

Figure 8: Block diagram of a Linear Quadratic Tracker

This design approach requires all the states to be available for control and the plant parameters A and B to be known [37]. This is the case in the model being used for this simulation. In a real-world scenario, it would not be difficult to make measurements of u (velocity in the x – direction), v (velocity in the y – direction) and r (the yaw rate) available to the controller. The control law is given by Equations (36) and (37). Equation (36) differs from Equation (35) by the inclusion of a gain $\mathbf{K_R}$ (acting on the reference) that modifies the control dynamics from that of a regulator to a tracker. **K** is the same as that obtained from the solution of the LQR problem. Equation (37) is the closed-loop dynamics of the system. $\mathbf{K_R}$ is given by Equations (38) and (39). Then, Q and R are the weighing matrices discussed in Section 2.3 and are initially chosen as 3 x 3 identity matrices. The system showed satisfactory performance with these values. The model was implemented in the SIMULINK environment. The block diagram of the setup is presented in Figure 9.

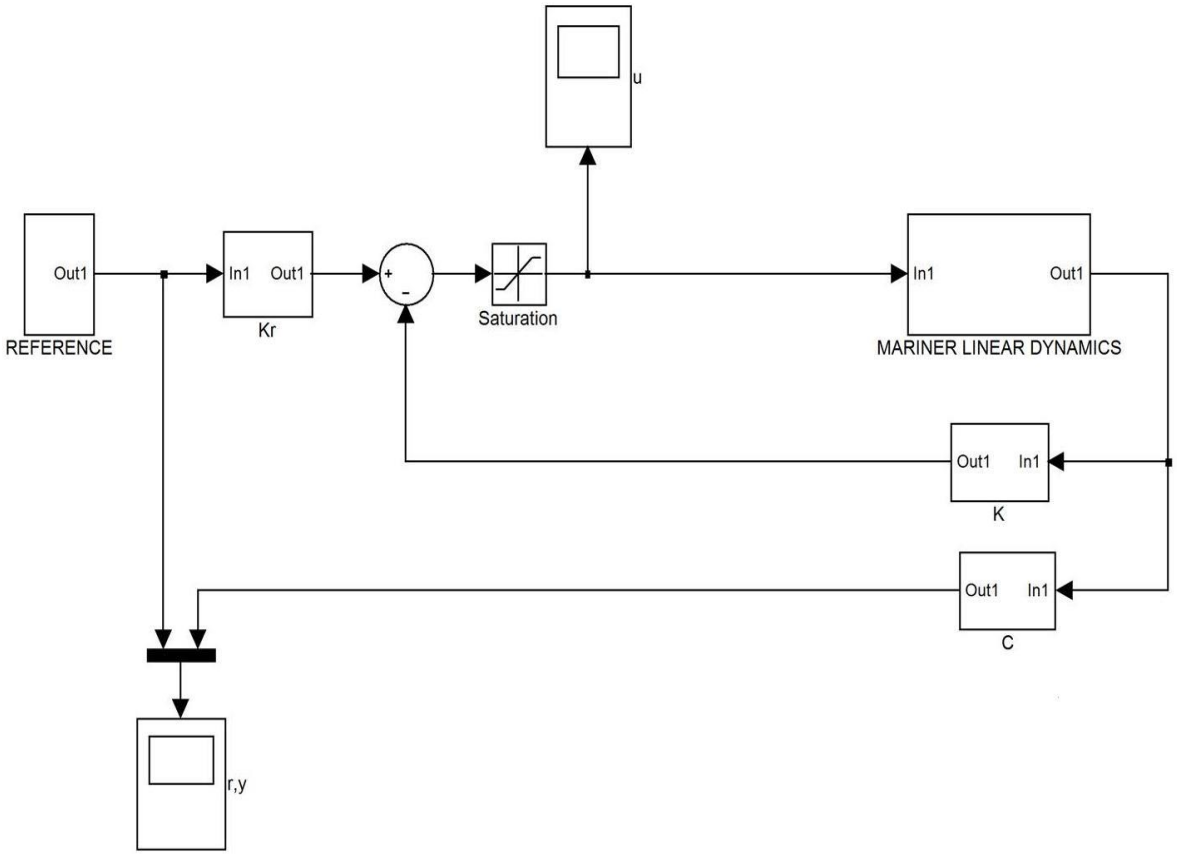

Figure 9: SIMULINK model of the control system design

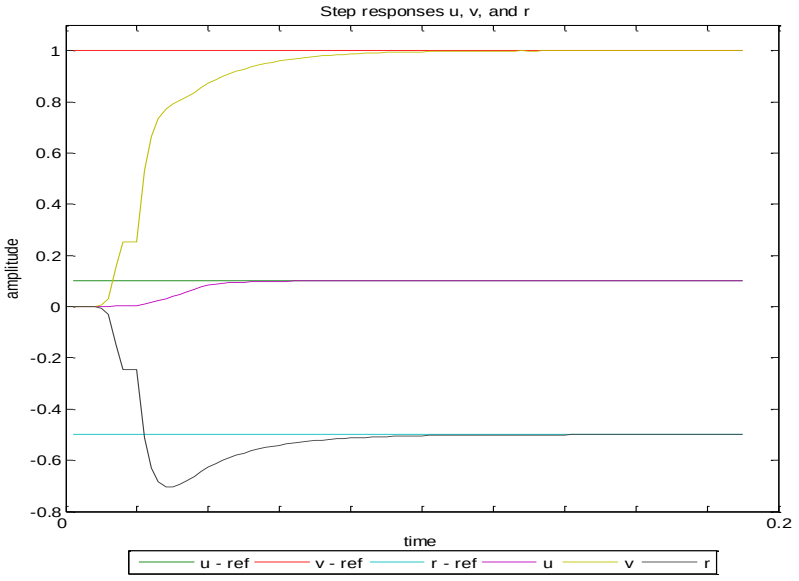

Figure 10: Step responses u, v and r of mariner's vessel over 0.2 seconds showing rapid convergence to reference values

Figure 10 represents the response for step inputs of 0.1, 1 and -0.5 to the three inputs u, v and r for 0.2 seconds. These plots show fast convergence to the step value for all the outputs indicating good tracking performance. Comprehensive plots of the system to different standard inputs are presented in the next section.

4. Results and discussion

4.1 Results

The following results are obtained from simulations in the MATLAB SIMULINK environment. See Appendices for the m – files used in creating the state space system and calculating the controller gains. It should be noted that the simulation time is not equivalent to real-time because of the normalization of the hydrodynamic parameters. The plots are hence presented in real-time by converting them with a factor equivalent to L/U, where L (160.93m) is the length of the vessel and U (7.7175m/s or 15 knots) is the nominal forward speed of the vessel as presented in the *mariner* m – file included in Tristan et al. [36]. Hence for every 1 second of simulation time, we have 20.85 seconds of real-time. The 5-second real-time plots provided correspond approximately to 0.24 seconds of simulation time. The plots are generated for different values of the LQR weighing matrices Q and R to show their relative importance in determining the speed and other transient characteristics of the response such as percentage overshoot, rise time, and settling time with reference inputs of 0.1, 1 and -0.5 for the x (surge) direction, y (sway) direction and the rotation N (yaw) about the z direction. These terms are collectively referred to as step response performance specifications [34] and are illustrated in Figure 11. Plots of the control inputs necessary to achieve the given step response performance are also provided to illustrate the controller action.

Figure 12 is derived for the following values of Q and R,

$$\mathbf{Q} = \begin{bmatrix} 1 & 0 & 0 \\ 0 & 1 & 0 \\ 0 & 0 & 1 \end{bmatrix},$$

$$\mathbf{R} = \begin{bmatrix} 1 & 0 & 0 \\ 0 & 1 & 0 \\ 0 & 0 & 1 \end{bmatrix}.$$

These give the controller gains of,

$$\mathbf{K} = \begin{bmatrix} 0.998 & 0 & 0 \\ 0 & 0.710 & 0.683 \\ 0 & -0.695 & 0.720 \end{bmatrix}, \qquad \mathbf{K_r} = \begin{bmatrix} 1.000 & 0 & 0 \\ 0 & 0.722 & 0.692 \\ 0 & -0.692 & 0.722 \end{bmatrix}$$

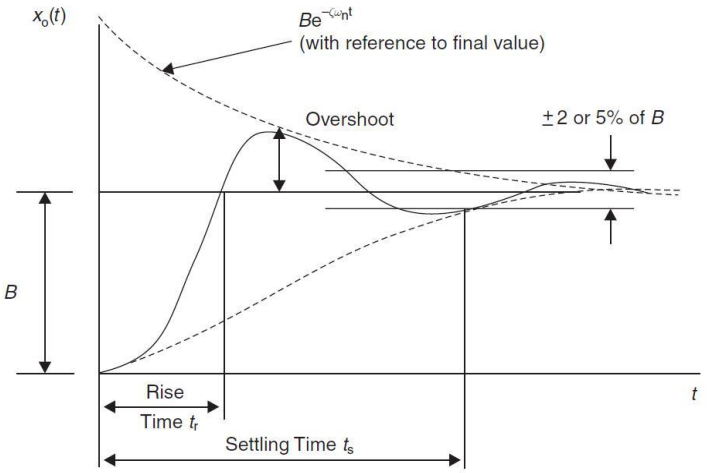

Figure 11: Step response performance specifications [37].

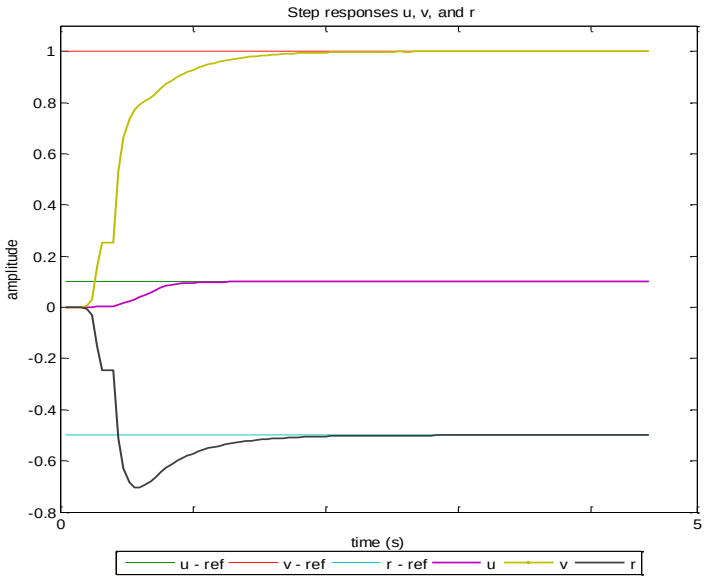

Figure 12: Step responses of mariner's vessel over 5 seconds

Table 3: Step response performance specifications for Figure 12

Specifications	u	v	R
Overshoot (%)	0	0	17.29
Rise time (s)	1.2	2.0	0.4
Settling time (s)	1.2	2.0	2.1

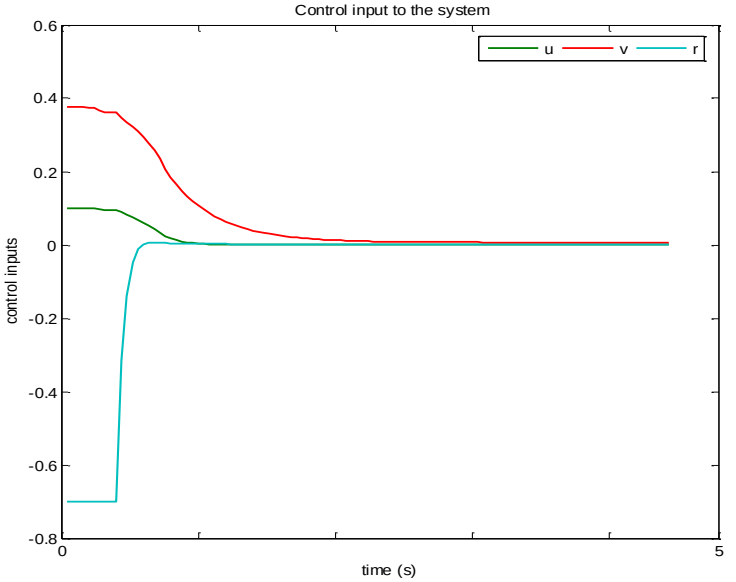

Figure 13: Control Inputs to the system to achieve the response of Figure 12

Essential details are also shown in Table 3, Figures 12 and 13. But Figure 14 was derived for the following values of Q and R chosen to illustrate the effect of increasing the values of the Q matrix coefficients. See also Table 4 for additional information related to Figure 14. In general the higher the value of the Q matrix coefficients, the faster the response since the feedback gain increases commensurately.

$$\mathbf{Q} = \begin{bmatrix} 50 & 0 & 0 \\ 0 & 50 & 0 \\ 0 & 0 & 50 \end{bmatrix},$$

$$\mathbf{R} = \begin{bmatrix} 1 & 0 & 0 \\ 0 & 1 & 0 \\ 0 & 0 & 1 \end{bmatrix}.$$

These give the controller gains of,

$$\mathbf{K} = \begin{bmatrix} 7.069 & 0 & 0 \\ 0 & 5.083 & 4.895 \\ 0 & -4.907 & 5.093 \end{bmatrix},$$

$$\mathbf{K_r} = \begin{bmatrix} 7.071 & 0 & 0 \\ 0 & 5.094 & 4.904 \\ 0 & -4.904 & 5.094 \end{bmatrix}$$

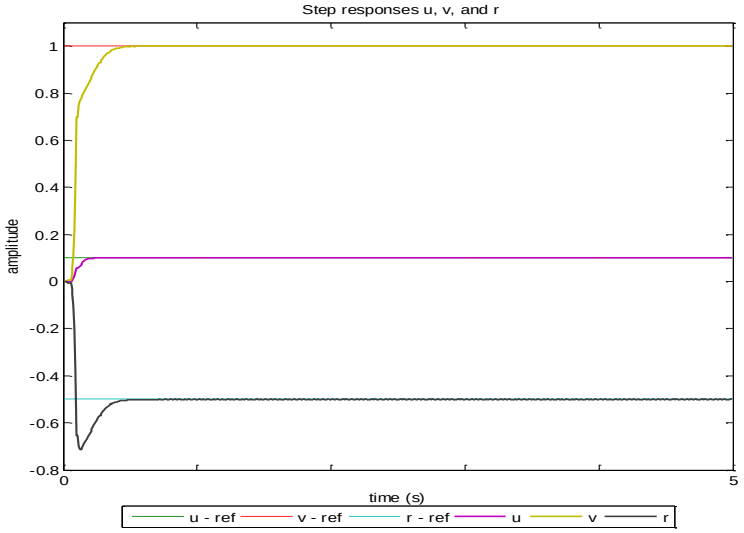

Figure 14: Step responses of mariner's vessel over 5 seconds showing the effect of increasing the feedback gains through Q

Table 4. Step response performance specifications for Figure 14

Specifications	U	V	R
Overshoot (%)	0	0	15.37
Rise time (s)	0.2	0.5	0.1
Settling time (s)	0.2	0.5	0.5

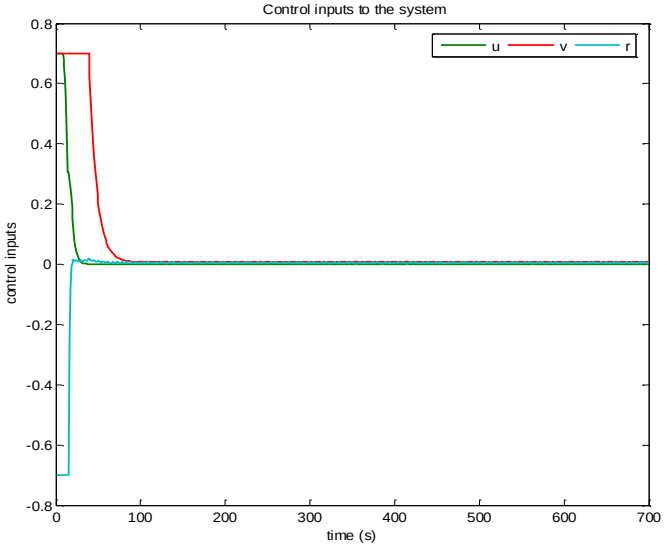

Figure 15. Control Inputs to the system to achieve the response of Figure 14

The effect of increasing the R matrix coefficients is to improve the damping characteristics of the controller at the expense of a reduction in the speed of the response. By choosing an appropriately high value, it was possible to eliminate the overshoot in the r (yaw) response as shown in Figure 16. See also Table 5.

$$\mathbf{Q} = \begin{bmatrix} 50 & 0 & 0 \\ 0 & 50 & 0 \\ 0 & 0 & 50 \end{bmatrix}, \qquad \mathbf{K} = \begin{bmatrix} 7.069 & 0 & 0 \\ 0 & 6.199 & 3.374 \\ 0 & -0.115 & 0.205 \end{bmatrix}$$

$$\mathbf{R} = \begin{bmatrix} 1 & 0 & 0 \\ 0 & 1 & 0 \\ 0 & 0 & 1000 \end{bmatrix} \text{ and } \qquad \mathbf{K}_r = \begin{bmatrix} 7.071 & 0 & 0 \\ 0 & 6.210 & 3.383 \\ 0 & -0.113 & 0.207 \end{bmatrix}$$

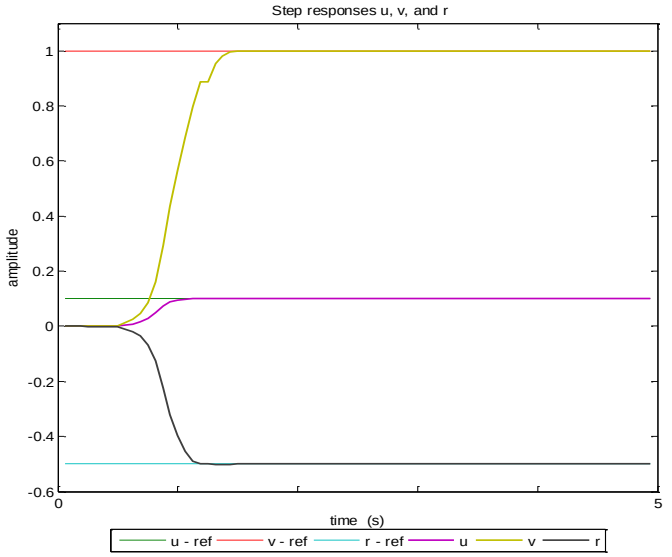

Figure 16. Step responses of mariner's vessel over 5 seconds showing the effect of increasing the R matrix coefficients

Table 5. Step response performance specifications for Figure 16

Specifications	u	v	R
Overshoot (%)	0	0	0
Rise time (s)	1.2	1.4	1.2
Settling time (s)	1.2	1.4	1.2

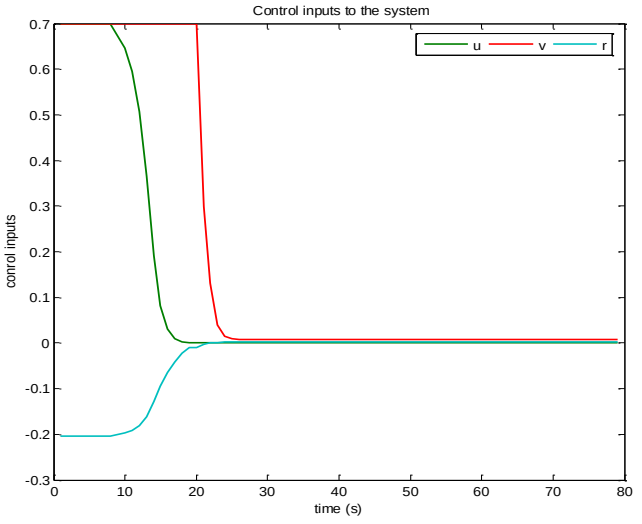

Figure 17: Control inputs to the system to achieve the response of Figure 14

To test the robustness of the controller, its response when measurement noise was introduced into the system was investigated. The noise was modelled as a Weiner process [38].

$$\dot{\varepsilon}(t) = \mathrm{n(t)} \tag{43}$$

$\dot{\varepsilon}(t)$ is the time derivative of the noise and,

$\mathrm{n(t)}$ is a random/stochastic function, in this case, band-limited white noise.

The plot of the response is shown in Figure 18. Using the same values of the Q and R matrices, the performance of the system to two other types of input; ramp and sinusoidal, was investigated. The reference weighting remains as before. The ramp input has a slope of 1. The response plots and the control inputs necessary to achieve them are presented in Figures 20 and 21. The sinusoidal input has a frequency of 30 rad/s. The amplitudes for u and r are 1 and 0.1 respectively. The amplitude for r is 0.5 but is 90 degrees out of phase with the other inputs. The plots of the reference and the control effort necessary to achieve this are presented in Figures 20 and 21.

As a final check of the controller's performance, the vessel's motion – due to a step response, in fixed or inertial coordinates X and Y was investigated. For a stable vessel, the resultant motion should be turning a full circle [26, 31]. The following plot, Figure 22 was obtained (see Appendices for SIMULINK block diagram of the time series generator). The axes are in meters and the motions have been converted from non-dimensional form by multiplying by L (160.93m). The equations for conversion from body-fixed coordinates to inertial coordinates are,

$$\left.\begin{aligned} \dot{x}_0 &= u\cos\psi - v\sin\psi \\ \dot{y}_0 &= u\sin\psi + v\cos\psi \end{aligned}\right\} \tag{44}$$

Once the two derivatives were evaluated, their integration gave the required time series motion.

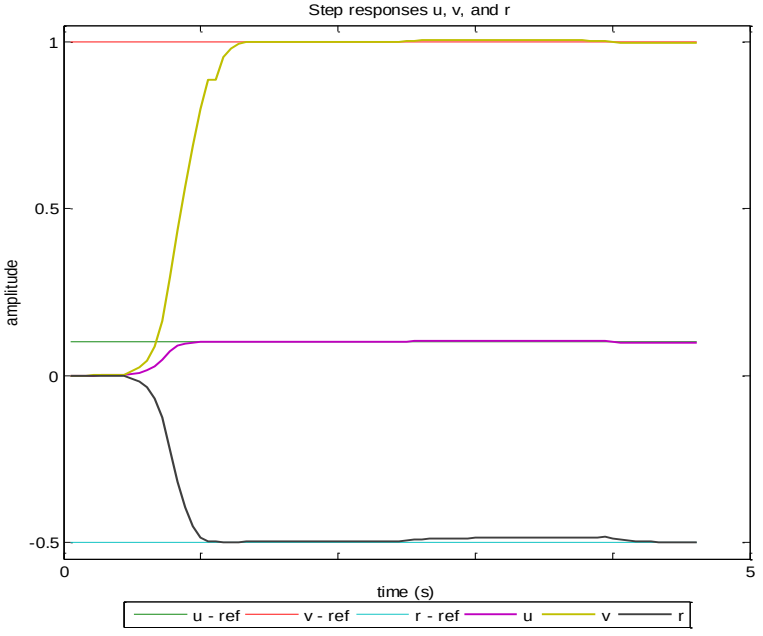

Figure 18. Step responses of mariner's vessel over 5 seconds showing controller performance with measurement noise

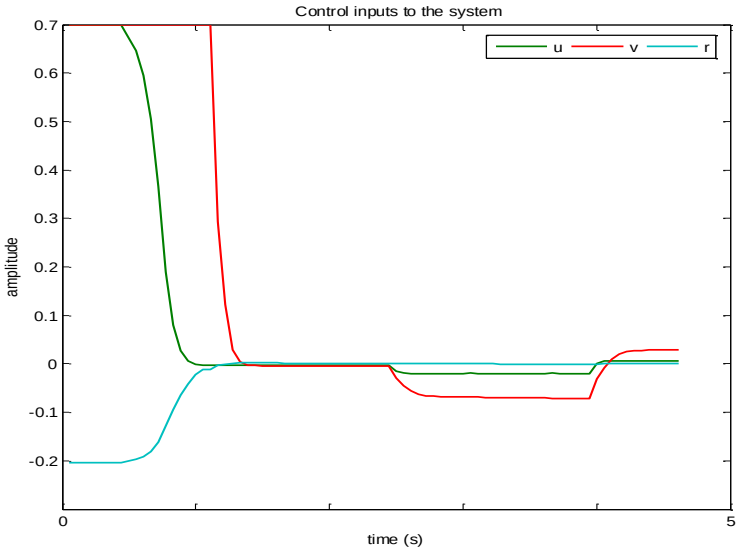

Figure 19: Control inputs to the system to achieve the response of Figure 18

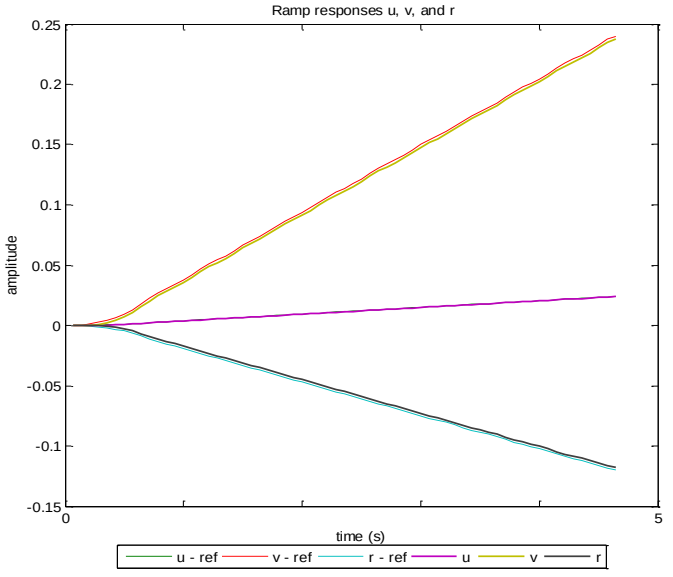

Figure 20: Ramp responses of mariner's vessel over 5 seconds showing minimal steady-state errors and mild oscillations in following the reference.

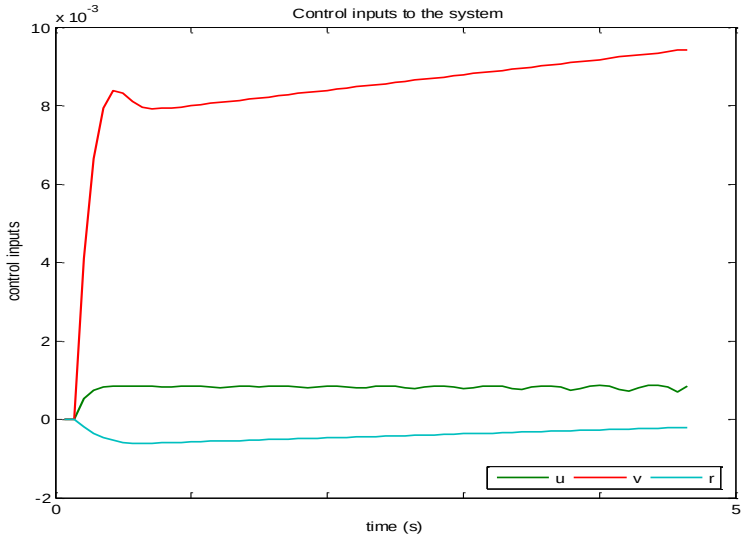

Figure 21: Control inputs to achieve the response of Figure 20

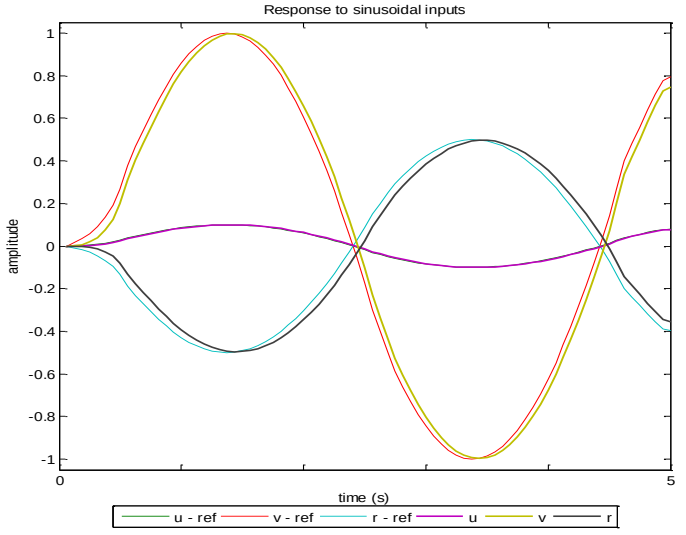

Figure 22: Responses of mariner's vessel to sinusoidal inputs over 5 seconds showing marked steady-state errors and practically no oscillations in following the reference.

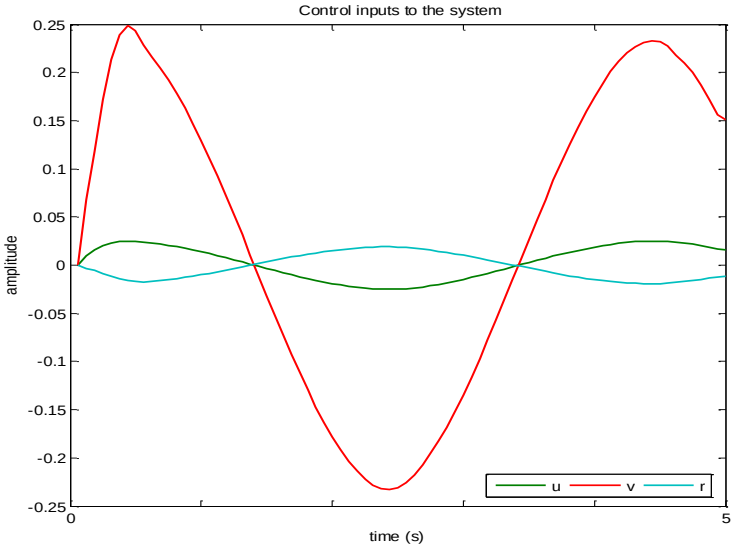

Figure 23: Control inputs to achieve the response of Figure 22

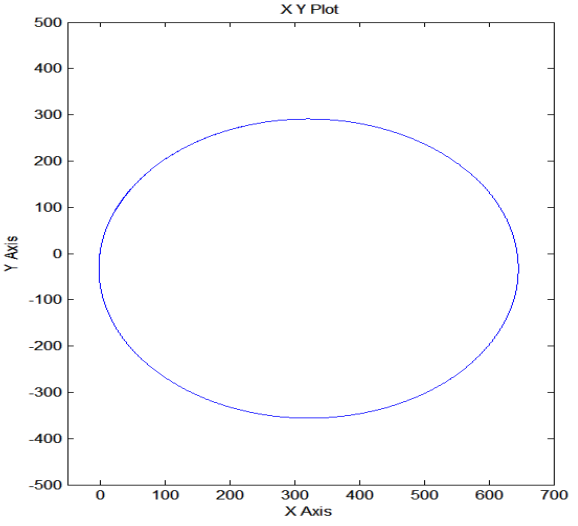

Figure 24. Mariner vessel executing a full turn as a response to a step rudder input over 3.5 minutes

4.2 Analysis of Results

There were two main objectives of controller design; stabilization of an unstable system and reference tracking. For stabilization, as Figures 12 to 20 indicate the controller was successfully able to achieve that aim. While Figure 6 shows rapidly diverging plots for step inputs, the plots in Figures 12 to 20 present a converging response indicative of a stable system. The reference tracking performance however varied depending on the choice of the controller gains. One other characteristic of a good control system is robustness in the presence of uncertainties. This was tested by introducing noise in the measurement of the system states, the control system still performed satisfactorily as shown in the plot Figure 8. However, there were minor oscillations in the step value.

Controller Performance Dependence on Q and R

Though the control inputs were unconstrained in the derivation of the optimization problem, a saturation block was used in the simulations to limit the control forces input into the system, this was to test the performance of the controller in a real situation

where there will be limits as to what values the control forces on the system can attain. It was found that increasing the controller gains through the values of the Q and R matrices used in solving the optimization problem generally gave better results though the Q and R matrices affected different parts of the response.

As shown in Figures 12 and 14, increasing the controller gains through the Q matrix increased the speed of the response. This was expected as the Q matrix weighs the relative cost of errors in the states of the system [31, 34]. Since increasing Q means that the errors are now very important, the optimization problem adapts to these constraints and tries to bring the errors to a minimum as fast as possible giving rise to faster settling times and rise times. In other words, the Q matrix determined how fast the system gets to the steady state. The R matrix on the other hand weighs the relative importance of the control effort on the cost optimization problem. As shown in Figure 16, increasing the coefficient of the R matrix that corresponds to the yaw (r) response eliminated the overshoot that was present in the response. The R matrix can then be seen as affecting the characteristics of the transient response at a penalty of increasing the settling and rise time as can be seen in the transition from Figure 14 to Figure 16 keeping the Q matrix constant and varying the R matrix. Depending on the limitations imposed by the physical system, which will vary from one vessel to the other, it is very possible to select the Q and R matrices to satisfy the needs of that particular application.

However, there will always be some form of steady-state error in the system (because of the absence of integrators) and this is the main setback of the design. In cases where the minimal steady-state error is not considered drastic (the errors are of a 10^{-2} order of magnitude for step inputs), the design gives a satisfactory response. If on the other hand, it is required that there should be no steady-state error whatsoever then integral action must be incorporated into the design to eliminate the error. This is at a cost of extra complexity in the system. For this design, however, the performance is very adequate.

For the response plots presented in Figures 18 and 20 which are for ramp and sinusoidal inputs respectively, the effect of the steady state errors becomes more noticeable. A ramp response can be used to simulate a steady change in the control forces. Sinusoidal inputs are usually not used in manoeuvring though they are sometimes used in full-scale testing of ships [26]. Again as stated in the preceding paragraphs, the error is relatively small. The states in the model are velocities and hence when a time series of the motion is obtained as shown in Figure 24, the vessel still performs in the expected manner i.e. turns a full circle [26, 31]. Due to the errors, however, it is possible that the vessel's turning radius or time varies from the actual one. Unfortunately, the amount of this deviation cannot be verified due to a lack of actual testing data for the vessel. For the simulation carried out on the model, the vessel has a turning radius of about 300m and completes a full turn in 3.5 minutes.

5. Conclusions

The work develops a Linear Quadratic Regulator based control system for stabilizing an unstable vessel model and tracking reference inputs with satisfactory performance. The control system has been tested with different values of its gains calculated for varying values of the Q and R matrices that are used in finding a steady-state solution to the matrix algebraic Riccati equation. The solution of this equation gives the feedback gain K of the Linear Quadratic Regulator problem. It was found that by choosing appropriate values for Q and R a finely tuned response can be obtained with no overshoots and a reasonable speed. This result is significant as it enables naval architects to design unstable hull forms which are generally easier to manoeuvre as long as their response can be guaranteed in a predictable way which is the effect of this controller design. Although Linear Quadratic Trackers have been used in ship control system design before, this design proceeds using an unstable vessel model as the starting point. The instability in the vessel model in this case is due to the limitations of the linear model. The linear model however is useful as the hydrodynamic parameters it is based on can be evaluated early on in the design. It is even possible to estimate them from statistical regression analysis based on the principal dimensions of the vessel such as those provided in Papoulias [26]. Thus, it allows designers to obtain some indication of how the vessel will perform and make necessary adjustments early on in the design. The work also proves the capability of the LQR design as a robust model capable of stabilizing an unstable system and giving it satisfactory step performance specifications.

The controller design presented here will usually form the core of either a dynamic positioning system or a ship autopilot system and will have to be combined with a control allocation algorithm to form a complete controller. The control allocation algorithm transforms the control signals from the

controller into physical actions performed by the control elements e.g. rudder, fins, etc.

To eliminate the effect of noise in the state measurements and errors due to environmental effects like winds etc, there will also be a need to incorporate a Kalman filter to find estimates of the system states and input these into the controller. This arrangement is usually referred to as a Linear Quadratic Gaussian (LQG) design. The combination of these three elements i.e. the Linear Quadratic Regulator/Tracker, the Kalman Filter, and the control allocation algorithm can then be implemented as a dynamic positioning system. For an autopilot, a means of incorporating Global Positioning System (GPS) measurements and probably weather forecasting data into the system will also be required.

Acknowledgements

We are grateful to the reviewers and editor of this journal for reviewing and publishing our work.

References

[1] Zou Y., Zhou X., Chen L., Xi X. "Impacts of different characteristics of marine biofouling on ship resistance," Ocean Engineering, Vol. 278, 2023, Article 114415. https://doi.org/10.1016/j.oceaneng.2023.114415

[2] Zoubir M., Gruner M., Franke T. "We go fast - It's their fuel": Understanding energy efficiency operations on ships and marine vessels," Energy Research & Social Science Vol. 97, 2023, Article 102992. https://doi.org/10.1016/j.erss.2023.102992

[3] Bayraktar M., Yüksel O. "Analysis of the nuclear energy systems as an alternative propulsion system option on commercial marine vessels by utilizing the SWOT-AHP method," Nuclear Engineering and Design, Vol. 407, 2023, Article 112265. https://doi.org/10.1016/j.nucengdes.2023.112265

[4] Onwuegbuchunam D.E., Akujuobi A.B.C. "SMEs financing and development in Nigeria's shipping sector: a case study," Advances in Management & Applied Economics, Vol. 3, No.6, 2013, pp. 143-157

[5] Ateme M.E. "Developing marine and coastal resources in Nigeria: Prospects and challenges," Maritime Technology and Research, Vol. 3, No. 4, 2021, pp. 335-347. DOI: 10.33175/mtr.2021.244473

[6] Bačkalov I. "Impact of contemporary ship stability regulations on safety of shallow-draught inland container vessels," Safety Science, Vol. 72, 2015, pp. 105-115. https://doi.org/10.1016/j.ssci.2014.09.001

[7] Liu R.W., Hu K., Liang M., Li Y., Liu X., Yang D. "QSD-LSTM: Vessel trajectory prediction using long short-term memory with quaternion ship domain," Applied Ocean Research, Vol. 136, 2023, Article 103592. https://doi.org/10.1016/j.apor.2023.103592

[8] Stępień B. "Can a ship be its own captain? Safe manning of autonomous and uncrewed vessels," Marine Policy, Vol. 148, 2023, Article 105451 https://doi.org/10.1016/j.marpol.2022.105451

[9] Piaggio B., Franceschi A., Villa D., Ferrari V., Tonelli R., Viviani M. "The heel influence on ship manoeuvrability: Single and twin-screw surface vessels," Ocean Engineering, Vol. 266, No. 1, 2022, Article 112721. https://doi.org/10.1016/j.oceaneng.2022.112721

[10] Xu L., Yang Z., Chen J., Zou Z. "Impacts of the COVID-19 epidemic on carbon emissions from international shipping," Marine Pollution Bulletin, Vol. 189, 2023, Article 114730. https://doi.org/10.1016/j.marpolbul.2023.114730

[11] Zhou X., Jing D., Dai L., Wang Y., Guo S., Hu H. "Evaluating the economic impacts of COVID-19 pandemic on shipping and port industry: A case study of the port of Shanghai," Ocean & Coastal Management, Vol. 230, 2022, Article 106339. https://doi.org/10.1016/j.ocecoaman.2022.106339

[12] Sakawa H., Watanabel N. "The impact of the COVID-19 outbreak on Japanese shipping industry: An event study approach," Transport Policy, Vol. 130, 2023, pp. 130-140. https://doi.org/10.1016/j.tranpol.2022.11.002

[13] Lucidi F.S., Semmler W. "Long-run scarring effects of meltdowns in a small-scale nonlinear quadratic model," Journal of Macroeconomics, Vol.75, 2023, Article 103487. https://doi.org/10.1016/j.jmacro.2022.103487

[14] Sutulo S., Soares C.G. "Review on ship manoeuvrability criteria and standards," Journal of Marine Science and Engineering, Vol. 9, No. 8, 2021, 904; https://doi.org/10.3390/jmse9080904

[15] Wang Z., Kim J., Im N. "Non-parameterized ship maneuvering model of deep neural networks based on real voyage data-driven," Ocean Engineering, Vol. 284, 2023, Article 115162. https://doi.org/10.1016/j.oceaneng.2023.115162

[16] Meng Y., Zhang X., Zhang X., Song C., "Weighted multi-kernel relevance vector machine for 3 DOF ship manoeuvring modeling with full-scale trial data," Ocean Engineering, Vol. 273, 2023, Article 113969, https://doi.org/10.1016/j.oceaneng.2023.113969

[17] Ayaz Z., Turan O., Vassalos D. "A 6 DOF manoeuvring model for controlled ship motions of POD-driven ships in Astern seas," IFAC Proceedings Volumes, Vol. 36, No. 21, 2003, pp. 193-198. https://doi.org/10.1016/S1474-6670(17)37806-0

[18] Taimuri G., Matusiak J., Mikkola T., Kujala P., Hirdaris S. "A 6-DoF maneuvering model for the rapid estimation of hydrodynamic actions in deep and shallow waters," Ocean Engineering, Vol. 218, 2020, Article 108103. https://doi.org/10.1016/j.oceaneng.2020.108103

[19] Delefortrie G., Vantorre M., "6DOF manoeuvring model of KCS with full roll coupling," Ocean Engineering, Vol. 235, 2021, Article 109327. https://doi.org/10.1016/j.oceaneng.2021.109327

[20] Wang L., Li S., Liu J., Hu Y., Wu Q. "Design and implementation of a testing platform for ship control: A case study on the optimal switching controller for ship motion," Advances in Engineering Software, Vol. 178, 2023, Article 103427. https://doi.org/10.1016/j.advengsoft.2023.103427

[21] Gopmandal F., Ghosh A., Kumar A. "LQ optimal robust multivariable PID control for dynamic positioning of ships with norm-bounded parametric uncertainties," Ocean Engineering, Vol. 266, No. 4, 2022, Article 113054. https://doi.org/10.1016/j.oceaneng.2022.113054

[22] Liu S., Roy S., Pairet-Garcia E., Gehrt J.-J., Siemer F., Büskens C., Abel D., Zweigel R., Case Study: Networked Control for Optimal Maneuvering of Autonomous Vessels, IFAC-PapersOnLine, Vol. 52, No. 8, 2019, pp. 440-445.

https://doi.org/10.1016/j.ifacol.2019.08.095
[23] Wang T., Skulstad R., Kanazawa M., Li G., Zhang H. "Knowledge transfer strategy for enhancement of ship maneuvering model," Ocean Engineering, Vol. 283, 2023, Article 115122. https://doi.org/10.1016/j.oceaneng.2023.115122
[24] Wei Z., Meng X., Li X., Zhang X., Gao Y. "Vessel manoeuvring hot zone recognition and traffic analysis with AIS data," Ocean Engineering, Vol. 266, No.1, 2022, Article 112858. https://doi.org/10.1016/j.oceaneng.2022.112858
[25] Lu S., Cheng X., Liu J., Li S., Yasukawa H. Maneuvering modeling of a twin-propeller twin-rudder inland container vessel based on integrated CFD and empirical methods, Applied Ocean Research, Vol. 126, 2022, Article 103261. https://doi.org/10.1016/j.apor.2022.103261
[26] Papoulias F. A., Ship Dynamics, 2000
[27] Tristan P., 2005, Ship motion control: course keeping and roll stabilisation using rudders and fins, Advances in Industrial Control, Springer London. https://doi.org/10.1007/1-84628-157-1
[28] SNAME. Nomenclature for treating the motion of a submerged body through a fluid JR. New York: Technical and Research Bulletin. 1952.
[29] Voight J. Quaternion Algebras, Springer Cham, pp. 1-885. https://doi.org/10.1007/978-3-030-56694-4
[30] Kuipers, J.B. Quaternions and Rotation Sequences: A Primer with Applications to Orbits, Aerospace, and Virtual Reality, Princeton University Press copyright 1999.
[31] Triantafyllou M.S., Hover F.S., "Manoeuvring and Control of Marine Vehicles," MIT Press, USA, 2003
[32] Skjetne R., Smogeli Ø.N., Fossen T.I., "A nonlinear ship manoeuvring model: identification and adaptive control with experiments for a model ship," Modelling, Identification and Control, Vol. 25, No. 1, 2004, pp. 3–27.
[33] Ogata K., Modern Control Engineering (4th Edition), Pearson Prentice Hall, UK 2002.
[34] Burns R.S., Advanced Control Engineering (1st Edition), Butterworth – Heinemann, UK, 2001.
[35] Lewis F.L., Vrabie D.L. and Syrmos V.L. Optimal Control, John Wiley & Sons, Inc., New Jersey, USA
[36] Tristan P., Smogeli O., Fossen T.I., Sørensen A.J. An overview of the marine systems simulator (MSS): A simulink toolbox for marine control systems, Modeling, Identification and Control, Vol. 27, No. 4, 2006. https://doi.org/10.4173/mic.2006.4.4
[37] "Mermaid propulsion unit". Wärtsilä. Retrieved 1 February 2020.
Youssef M. M., El-Shenawy A.K., Elsingaby M. Trajectory following and stabilization control of fully actuated AUV using inverse kinematics and self-tuning fuzzy PID, PLoS ONE, Vol. 12, No. 7, 2017. DOI: 10.1371/journal.pone.0179611
[38] Duan J., Wang W. Effective Dynamics of Stochastic Partial Differential Equations, Chapter 3 - Stochastic Calculus in Hilbert Space, 2014, pp. 21-47. https://doi.org/10.1016/B978-0-12-800882-9.00003-2

Appendix 1
SIMULINK block diagram of the time series generator.

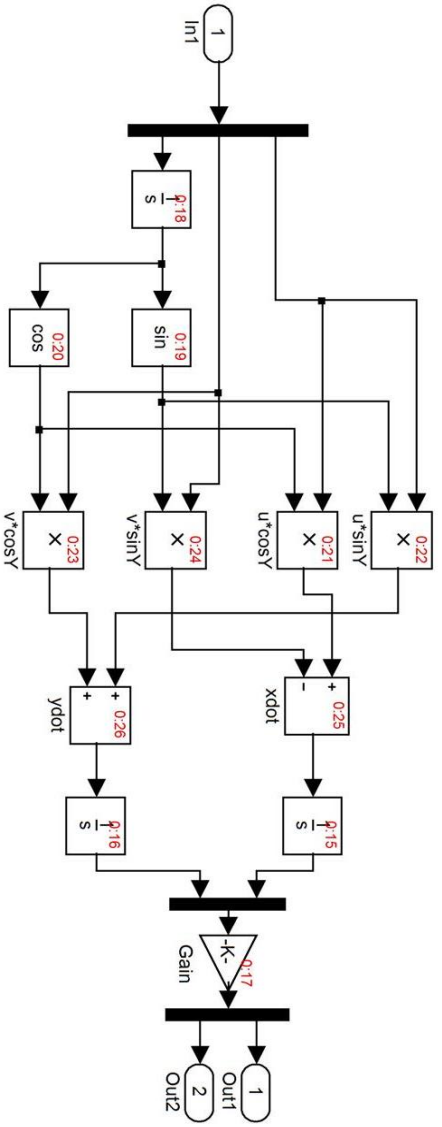

v_mariner.m: MATLAB script to generate state space model

Appendix 2

10/11/07 16:48 C:\MATLAB7\work\v mariner3.m 1 of 3

```
%The script below generates a state space model for
%a vessel using linear approximation (Taylor's expansion)
%of the sway-yaw manoeuvering model.
%
%Author:        Owolabi Oluseye
%               Mechanical Engineering Department
%               University of Lagos
%
%References:    Maneuvering and Control of Marine Vehicles
%               M.S. Triantyafyllou and F.S. Hover
%
%Data Source:   Marine GNC (mariner m-file)
%               Trygve Lauvdal
%
%The data below is for a Mariner class vessel. Normalized values are used
%for the hydrodynamic coefficients.

m = 798e-5; %Mass of vessel

xG = -0.023; %x-coordinate of CG

Iz = 39.2e-5; %Moment of Inertia about Z axis

U = .5; %Forward speed

Xudot =  -42e-5;

Xu    = -184e-5;

Yvdot =  -748e-5;

Yrdot = -9.354e-5;

Nvdot = 4.646e-5;

Nrdot = -43.8e-5;

Yv = -1160e-5;

Yr = -499e-5;

Nv = -264e-5;

Nr = -166e-5;

%The following line determines the suitability of a linear model

C = (Nr  - m*xG*U)*Yv - (Yr - m*U)*Nv;

if C < 0
```

10/11/07 16:48 C:\MATLAB7\work\v mariner3.m 2 of 3

```
   warning ('A non-linear model will be more appropraite.The vessel model generated
is unstable...')

end

%The following lines calculate the state space matrices

disp('Calculating state-space matrices...')

M11 = m - Xudot;

M12 = 0;

M13 = 0;

M21 = 0;

M22 = m - Yvdot;

M23 = m*xG - Yrdot;

M31 = 0;

M32 = m*xG - Nvdot;

M33  = Iz - Nrdot;

M = [M11 M12 M13; M21 M22 M22; M31 M32 M33];

P11 = Xu;

P12 = 0;

P13 = 0;

P21 = 0;

P22 = Yv;

P23 = Yr - m*U;

P31 = 0;

P32 = Nv;

P33 = Nr - m*xG*U;

P = [P11 P12 P13; P21 P22 P23; P31 P32 P33];
```

10/11/07 16:48 C:\MATLAB7\work\v mariner3.m 3 of 3

```
a = inv(M)*P;

b = inv(M);

c = eye(3);

d = [0];

%It is assumed there is no direct feed in the system.

mariner_ss3 = ss(a,b,c,d)
```

Appendix 3

vessel_response_lqr3.m: MATLAB script for creating SIMULINK optimal controller variables.

10/11/07 17:07 C:\MATLAB7\work\vessel response lqr3.m 1 of 1

```
%M file that creates variables for the simulations
%
%Author:        Owolabi Oluseye
%               Mechanical Engineering Department
%               University of Lagos
%

disp('Calculating K,Kr the LQR optimal feedback matrices...')

Q = [50 0 0; 0 50 0; 0 0 50];

R = [1 0 0; 0 1 0; 0 0 1000];

k = lqr(a,b,Q,R)

kr = -inv(c*inv(a-b*k)*b)
```